

Green Synthesis, Characterization and Antimicrobial, Antifungal properties of *Butea monosperma* Mediated Silver Nanoparticles.

Akshay Milind patil*, Sonali Das

PhD Research Scholar, Centre of Biotechnology, Pravara Institute of Medical Sciences (DU)
Loni, 413736 (M.S.) India,

Abstract:

Silver nanoparticles are deemed the most positive, considering their strong volume surface region, and is of concern for study because of the improved microbial tolerance to antibiotics and medicines. Therefore, green synthesis of nanoparticles of silver using biomolecules derived from various plant sources in the form of extracts can be applied for the screening of different diseases which trigger microorganisms and for the physical and biological characterisation of plant-derived silver nanoparticles. The experiment involved the green synthesis of silver nanoparticles (AgNPs) from *Butea monosperma* leaf extract. Biosynthesized *Butea monosperma* -AgNPs were characterized by UV-visible spectroscopy, fourier-transform infrared (FTIR) spectroscopy and scanning electron microscopy (SEM). The intensity of peak broad range 200-800nm in UV-vis spectra, EDS test. The SEM shows the actual size of the nanoparticles. Antibiotic-resistant bacteria and fungus have surprisingly increased over recent years. the rate of development of new antibiotics to treat these emerging issues is very slow. Therefore, the aim of this study was to prepare novel nanoparticles formulations to improve the antimicrobial and antifungal activities. In the present work, I have attempted to test the prepared nanomaterials against multiple gram negative and gram-positive microbial strains, Antibacterial activity against *Shigella* *Salmonella typhi*, *Echerichia coli*, *Staphylococcus aureus*, *Pseudomonas aeruginosa*, *Acinetobacter*, *klebsiella pneumoniae*, *Bacillus subtilis* as

well as fungal strains *Aspergillus Niger*, *Aspergillus Oryzae*, *Candida albicans*, *Penicillium crysogenum* and *Aspergillus flavus* causing harmful disease and infections Well plate diffusion Method

(Key words: Nanoparticles, *Butea monosperma*, AgNPs, UV-visible spectroscopy, fourier-transform infrared (FTIR) spectroscopy and scanning electron microscopy (SEM), *Staphylococcus aureus*, *Oryzae*, *Candida albicans*, *Aspergillus flavus*)

INTRODUCTION

Bacterial infections are the second acknowledged cause of death worldwide and the third in developed countries. The therapeutic efficiency of antimicrobials has become more complex due to the emergence of multidrug resistance. (Hwang *et al.* 2016.) *B. monosperma* has numerous pharmacological activities such as anthelmintic, anti-conceptive, anticonvulsive, antidiabetic, antidiarrheal, antiestrogenic and antifertility, anti-inflammatory, antifungal, antibacterial, antistress, anticancer, antioxidant, chemopreventive, haemagglutinating, hepatoprotective, thyroid inhibitory, antiperoxidative, hypoglycemic effects, wound healing activities, anti-giardiasis, antifertility, chemo preventive activities and radical scavenging activities (Sindhia *et al.*, 2010 More *et al.*, 2012 Sharma and Deshwal 2011 Chandraker 2014 Madhavi 2013) *Candida albicans* is commonly found as a commensal fungus in the mucosa lining of humans. Normally, this organism does not provoke immune responses in individuals with a normal immune function. When the immune system fails and the host's environment changes, infections can develop that are superficial to life-threatening. A high rate of mortality and morbidity is associated with systemic candidiasis. As much as 10-24% of patients with invasive Candidiasis die. This opportunistic pathogen can survive on abiotic surfaces for up to four months. As a result of its ability to form biofilms and change its morphology, the organism can survive on abiotic surfaces. An extracellular matrix surrounds polymorphic cells (yeast, hyphal, pseudo-hyphal cells) of this organism. The extracellular matrix contains proteins, polysaccharides, glycerolipids, and DNA. Extracellular DNA is essential for establishing structural integrity of the biofilm and safeguarding it from external agents, such as antifungal therapeutics. Additionally, it prevents the penetration of antifungal agents

into the biofilm. In addition to colonizing medical devices such as catheters, pacemakers, prosthetics, and other abiotic surfaces, biofilms may act as reservoirs for pathogenic cells. Biofilms are inherently resistant to antimicrobial agents because of their composition. Therefore, disrupting the biofilm might be crucial to infection treatment. *C. albicans* pathogenesis relies heavily on biofilms, so novel strategies to inhibit and disrupt the formation of biofilms are needed. Scientists are considering nanotechnology as a possible strategy to inhibit *Candida* biofilms. Physico-biological concepts are integrated in nanotechnology for the development of novel therapies.

A common cause of catheter-associated urinary tract infections (CAUTIs) is *Proteus mirabilis*, a Gram-negative bacterium. Infections caused by such bacteria are mainly caused by the formation of biofilms on catheter surfaces. Virulence factors expressed by *P. mirabilis* are necessary for forming biofilms. Factors such as adhesion molecules, quorum sensing molecules, lipopolysaccharides, efflux pumps and urease enzymes may be involved in this process. Developed on catheter surfaces, *P. mirabilis* biofilms have the unusual characteristic of being crystalline due to their ureolytic biomineralization. The result is catheter encrustation and blockage, often accompanied by urine retention and ascending UTIs. Bacteria embedded in crystalline biofilms become highly resistant to conventional antimicrobials as well as the immune system. Being refractory to antimicrobial treatment, alternative approaches for eradicating *P. mirabilis* biofilms are urgently required. The term nanomaterial refers to materials with a diameter smaller than 100 nanometers. Among the traditional methods used to synthesize these nanoparticles are precipitation, wet chemical synthesis, sol-gel, and pyrolysis. However, these methods are highly energy-intensive and, therefore, not environmentally friendly. In the present work, we have attempted to test the as-prepared nanomaterials against the biofilm of *C. albicans* and *P. mirabilis*. *Proteus mirabilis* is a common pathogen responsible for complicated urinary tract infections (UTIs) that sometimes causes bacteremia. Most cases of *P. mirabilis* bacteremia originate from a UTI. Candidiasis is a fungal infection caused by a yeast (a type of fungus) called *Candida*. Some species of *Candida* can cause infection in people; the most common is *Candida albicans*. *Candida* normally lives on the skin and inside the body, in places such as the mouth, throat, gut, and vagina, without causing any problems. *Candida* can cause infections if it grows out of control or if it enters deep into the body (for example,

the bloodstream or internal organs like the kidney, heart, or brain). (Chi-Yu Chena *et al.*, 2012). Metals such as metals and metal oxides, silicates, non-oxide ceramics, polymers, organic materials, biomass and biomolecules may be used for producing nanoparticles. In many morphologies, nanoparticles occur, including balls, cylinders, platelets, tubes etc. Inorganic nanoparticles such as golden and silver metal nanoparticles have superior material properties with mechanical flexibility, with broad availability, comprehensive mobility, strong compatibility, selective therapeutic products and regulated drug release capabilities (Xu *et al.*, 2006). For the synthesising and stabilisation of silver nanoparticles, many physical, chemical and biological methods were used (Senapati *et al.*, 2005). The word biofilm has been used to refer to the thin coated condensations of microbes (for example bacteria, fungi, protozoa, etc.) which can appear in different types of surface structures. Antifungal performance may be calculated by means of well diffused methods on various fungal strains. (Chitte *et al.*, 2016) Free floating bacteria, classified as planktonic microorganisms in an aqueous climate, are a requirement for the development of biofilms. Thus, such films may be formed on every organic or inorganic substratum where planktonic microorganisms prevail in a water solution (Choudhary *et al.*, 2012). Because of its unusual physical and chemical properties, silver nanoparticles (AgNPs) are progressively being used in numerous fields, including medical, fruit, patient treatment, consumption and industrial uses. This involves visual, electronic, thermal, heavy electrical and biological characteristics (Gurunathan *et al* 2015). Because of its unusual properties, it has been used for many applications in the medicinal, food processing, surgical, orthopaedic, medication distribution, anticancer industries, as well as for numerous applications such as non-bacterial agents, automotive, domestic and health goods, electronic products, medical equipment jackets, optical sensors and cosmetics AgNPs have been widely used lately in numerous textiles, keyboards, wound dressings and biomedical instruments. The nanosized metallic particles are peculiar and, because of their surface to volume ratio, can greatly alter physical, chemical and biological properties; thus, nanoparticles have been used for different purposes. In order to satisfy the AgNPs criterion, different methods for synthesis have been introduced. In general, current approaches of physics and chemistry appear rather costly and risky. It is important to notice the high yield, solubility and high stability of biologically prepared AgNPs (Gurunathan *et al.*, 2015). Biological methods for

AgNPs seem simplistic, quick, nontoxic, reliable and green among. A range of analytical methods are used, including UV spectroscopy, X-ray diffractometry (XRD), Fourier transform infrared spectroscopy (FTIR), X-ray photoelectron spectroscopy (XPS), DLS scanning, SEM, transmission electron microscope (TEM), atomic force microscopy (AFM). Several competent books and studies have identified different styles of methodological methods for characterising AgNPs. A highly effective and accurate technique for the primary characterization of synthesised nanoparticles used for tracking the production and stabilisation of AgNPs is UV-Visible Spectroscopy. (Sastry *et al.*, 1998).

1. Materials and methods

1.1 Sample preparation: The young and disease-free leaves of *Butea monosperma* were selected.

Drying of leaves: Samples were dried in room temperature for more than two weeks, so that they may be converted into fine powder.

Preparation of fine powder: after proper drying of leaves, thick mid ribs of the leaves were removed, dried leaves were grinded into fine powder using a grinder.

Preparation of extracts: aqueous extracts using distilled water, 50% ethanol, 50% methanol & 50% acetone were prepared.

1.2 Synthesis of Silver Nanoparticles from *Butea monosperma* extracts:

AgNPs were synthesized by the following method. 10mM AgNO₃: plant extracts in different solvent in 9:1 ratio in a reagent bottle mixed thoroughly, forming a uniform mixture. The mixture was then rested at room temperature for 24 hours at 37°C, with continuous monitoring. After about few minutes, the mixture was observed to start changing from pale green to yellowish brown. After about 24 hours, the mixture had completely changed colour to brown in all solvents. This color change is visual evidence of formation of AgNPs. (Kasthuri *et al.*, 2009).

1.3 Characterization of silver nanoparticles.

For determination of the time point of maximum production of silver nanoparticles, the absorption spectra of the samples were taken 200–8000 nm using a UV–vis spectrophotometer. The silver nanoparticles were synthesized by novel green chemical route. The nanoparticles were characterized by

UV- spectral analysis, SEM -EDAX analysis (Scanning Electron Microscopy) was performed for studying the surface morphology & to predict the size of the nanoparticle. Also, FTIR analysis was conducted for identifying the presence of functional groups. (Anuja *et al.* 2020)

2. **Antibacterial activity** (Moonmun, *et al.*, 2017)

Antibacterial activity against different bacteria by Well plate diffusion Method. The inoculum of the microorganism was prepared from the bacterial cultures. 15ml of nutrient agar medium was poured in clean sterilized Petri plates and allowed to cool and solidify. 100 µl of broth of *Shigella Salmonella typhi*, *Echerichia coli*, *Staphylococcus aureus*, *Pseudomonas aeruginosa*, *Acinetobacter*, *klebsiella pneumoniae*, *Bacillus subtilis* strain was pipette out and spread over the medium evenly with a spreading rod till it dried properly. Wells of 6mm in diameter were bored using a sterile cork borer. Solutions of all the *Butea monosperma* AgNPs different solvents (25,50,75) % in DMSO were prepared. 100µl of plant extracts solutions was added to the wells. The petri plates incubated at 37⁰C for 24 h. streptomycin (1mg/ml) was prepared as a positive control DMSO was taken as negative control.

Antifungal activity (Umadevi *et al.*, 2003)

Stock solution for antifungal activity: For antifungal study each compound was dissolved in DMSO at a concentration of 5mg/ml and stored in a refrigerator till further used. Antifungal activities of the compounds were evaluated by means of agar well diffusion assay. The assay was carried out according to the method of (Hufford *et al.*, 1975). Sabouraud dextrose agar was used for the growth of fungus. Media with acidic pH (pH 5.5 to 5.6) containing relatively high concentration of glucose (40%) is prepared by mixing (SDA) Sabouraud dextrose and distilled water and autoclaved at 121°C for 15 minutes. 25 ml of molten (45⁰C) SDA medium was aseptically transferred into each 100mm×15mm sterile Petri dish. For counting of spore (fungi)

were suspended in normal saline to make volume up to 1ml and then counted with help of hemacytometer (neubar chamber). Once the agar was hardened, 8mm wells were bored using a sterile cork borer. Then 0.1ml (100µl) from each stock solution of the compounds having final concentration of 5mg/ml was placed in each the well and the plates were incubated for 24 hour at 29°C. Two wells in each petri dish were supplemented with DMSO and reference antifungal drug Clotrimazole (1mg/ml) dissolved in DMSO serve as negative and positive control respectively.

3. Antimicrobial and antifungal study using MTT Assay: (Tereza 2018)

Candida albicans and *Proteas mirabilis* was procured from culture collection centre.

Both cultures were routinely maintained on Yeast peptone dextrose broth (Himedia make). YPD and Luria Bertani (Himedia Make) LB broth. Yeast peptone dextrose broth is prepared by dissolving the 50 g powder of YPD media into 1000 mL distilled water and the prepared media was autoclave at 15 pounds per square inch to achieve a chamber temperature of at least 250°F (121°C) for a prescribed time—usually 10–15 minutes. YPD was used for growing fungal cells. For antimicrobial activities, Initially, 100 µl volume of each culture with 1.0 OD in RPMI media was aseptically added, separately, and a mixture as well into 96 well plate containing various volumes (0-10 µl) of different nanoparticles, viz., A-Y, B-Y, C-Y and D-Y in 96 well plate and incubated at 37°C. After incubations, 10 µl of 10 mg/ml MTT solution was added in each well, and plate was incubated for 2 hours in dark at 37°C. After incubation, 100 µl DMSO were added to each well and the solutions in each well was read at 570 nm on multimode plate reader. Control samples were without nanoparticles under similar conditions

3) RESULT & DISSCUSSION

3.1) The detailed study on biosynthesis of silver nanoparticles by natural *Butea monosperma* extracts such It was observed that the color of the solution turned from yellow to bright yellow

and then to dark brown after 1,24 and 48 h of the reaction, which indicated the formation of silver nanoparticles (fig 1).

3.2) The formation and stability of the reduced silver nanoparticles in the colloidal solution was monitored by UV–vis spectrophotometer analysis. The UV–vis spectra show maximum absorbance at 420 nm, which increased with time of incubation of silver nitrate with the plants extract. The curve shows increased absorbance in various time intervals (1 h, 24 h and 48 h) and the peaks were noticed at 420 nm corresponding to the surface plasmon resonance of silver nanoparticles. The observation indicated that the reduction of the Ag⁺ ions took place extracellularly. It is reported earlier that absorbance at around 430 nm for silver is a characteristic of these novel metal particles (Nestor *et al.*, 2008). The synthesis of AgNPs from the ethanolic, aqueous, methanol & acetone extract of leaves of *Butea monosperma* was further confirmed by ultraviolet - visible spectroscopy (UV/VIS) in the range of between 200 nm to 800 nm and solvents were used as a blank. The spectrum has a maximum absorption peak at a which is reported to have an absorption maximum of between about 400nm to about 450nn. The presence of the maximum peak absorption peak at 400nm to about 450nn is therefore an indication and confirmation that the AgNPs were present. (Fig 1)

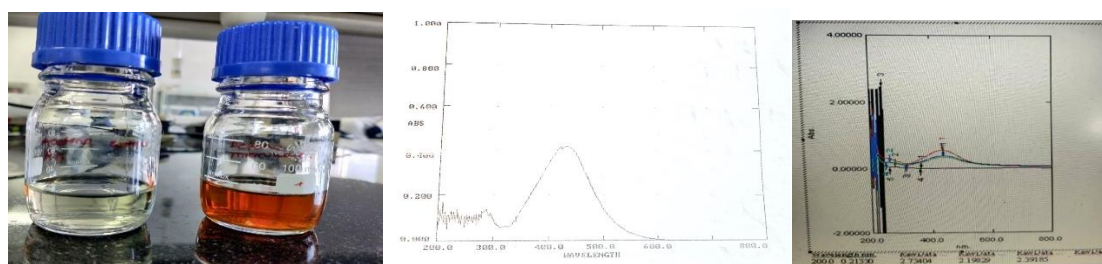


Fig 1. Synthesis of nanoparticles & presence of the maximum peak absorption peak at 400nm to about 450nn

3.3) Fourier Transform Infra-Red Spectrometer (Equipped With ATR) Model Tensor 600 Bruker. As seen in figure given below, FTIR spectra of all samples shows similar pattern.

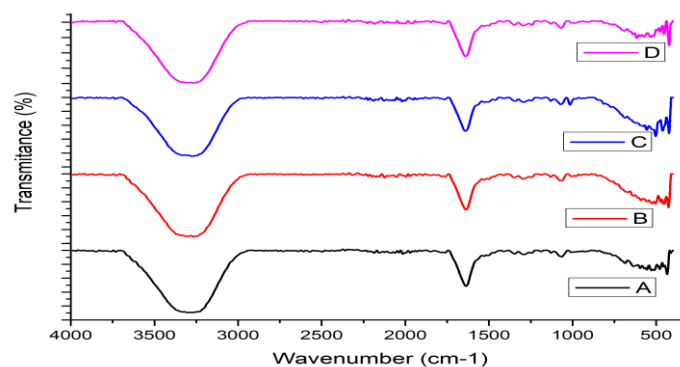


Fig 2. FTIR spectra of all four solvents of *Butea monosperma* synthesized Silver AgNPs

FTIR spectra depicts bands at ~3200-3300 corresponding to alcoholic O-H stretching, bands at ~ 1620 corresponds to; where as small band at ~1100 is corresponds to alcoholic C-O bond, metallic silver bond is seen at ~450 cm⁻¹. Fig 2 where A-water, B Ethanol, C methanol & D acetone solvents respectively.

3.4) Field Emission Scanning Electron Microscopy (Fe-SEM) & Energy Dispersive X-Ray spectroscopy (EDS) Analysis. Thin film of the as obtained sample was prepared on cleaned glass plate using drop casting technique. This film is dried under Infra-Red lamp at room temperature. As depicted in electron micrographs, sample consist of clusters of ultrafine nanoparticles of size ~40-75 nm. Fig 4 To confirm the composition of the sample, EDS analysis is done. As

Seen from the spectra depicted in chart 1, Sample prominently consist of Ag along with S, P, O and Si.

Table 1. Elemental composition of as synthesized sample					
Element	Atomic No	A	B	C	D
Carbon	6	23.81	20.64	19.07	22.53
Aluminum	13	10.18	ND	ND	ND
Silver	47	47.10	45.49	44.70	45.60
Sulfur	16	5.20	ND	ND	ND
Phosphorus	15	1.50	ND	ND	ND
Silicon	14	1.23	ND	ND	ND
Oxygen	8	10.98	9.91	36.24	31.88

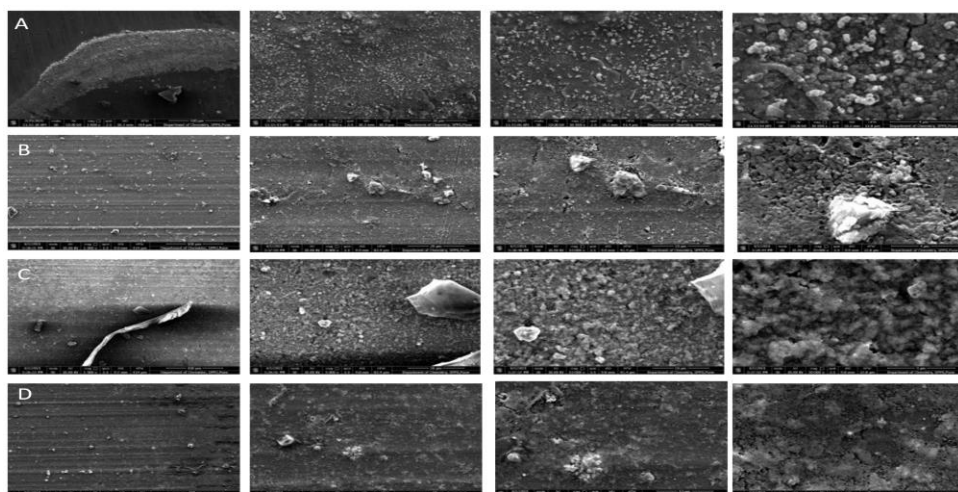


Fig 3 Field Emission Scanning Electron Microscopy (Fe-SEM)

3.5) Antibacterial activity was evaluated by measuring the diameters of the zone of inhibitions (ZI) all the determination were performed in triplicates. *Shigella* *Salmonella typhi*, *Echerichia coli*, *Staphylococcus aureus*, *Pseudomonas aeruginosa*, *Acinetobacter*, *klebsiella pneumoniae*, *Bacillus subtilis* were studied as follows.

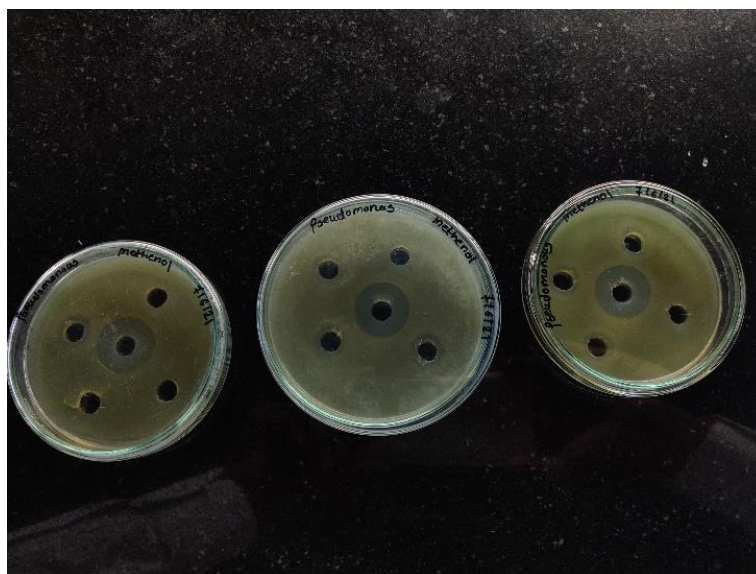


Fig 4: activity against *Pseudomonas aeruginosa*

		Ethanol	Methanol	Water	Acetone
<i>Staphylococcus aureus</i>	Standard antibiotic(mm)	31.33	31	17.66	17
	25% (mm)	12.33	14.33	15.66	13
	50% (mm)	16	15.33	17.33	16
	75% (mm)	17.66	17	18.33	17.33
<i>Pseudomonas aeruginosa</i>	Standard antibiotic(mm)	12.33	24	24.33	24.33
	25% (mm)	11	11.33	10.33	14.66
	50% (mm)	16	12.66	12.66	16.33
	75% (mm)	19.66	14.66	15.33	18.66
<i>Ancientobactes</i>	Standard antibiotic(mm)	25.66	26	25	26
	25% (mm)	12.33	14	12.33	10.66
	50% (mm)	14	16.33	15.33	12.66
	75% (mm)	16.66	18.33	17.33	15
<i>Klebsiella Pneumonia</i>	Standard antibiotic(mm)	23	22.66	21.33	24
	25% (mm)	10	-	-	-
	50% (mm)	12.33	-	-	-
	75% (mm)	13	-	-	-
<i>Bacillus subtilis</i>	Standard antibiotic(mm)	31.33	31	29	30
	25% (mm)	-	-	-	-
	50% (mm)	-	-	-	-
	75% (mm)	-	-	-	-
<i>Escherichia coli</i>	Standard antibiotic(mm)	15	15	15	15
	25% (mm)	08	06	08	09
	50% (mm)	08	07	09	06
	75% (mm)	08	06	08	08
<i>Salmonella Typhi</i>	Standard antibiotic(mm)	24	24	24	24
	25% (mm)	06	09	09	06
	50% (mm)	09	08	08	09
	75% (mm)	10	12	11	11
<i>Shigella</i>	Standard antibiotic(mm)	24	25	24	26
	25% (mm)	10	10	10	-

	50% (mm)	10	11	10	-
	75% (mm)	10	12	13	06

Result: At the concentration 1 mg/ml, the SAMPLES A, B, C, D showed moderate activity against *Pseudomonas aeruginosa*

3.6) The antifungal activity was measured as the diameter (mm) of clear zone of growth inhibition. Antifungal activities of the compounds were evaluated by means of agar well diffusion assay. *Aspergillus Niger*, *Aspergillus Oryzae*, *Candida albicans*, *Penicillium crysogenum* and *Aspergillus flavus* were studied as follows. Table no : Antifungal study of *Butea monosperma* AgNPs on : *Aspergillus Niger*, *Aspergillus Oryzae*, *Candida albicans*, *Penicillium crysogenum* and *Aspergillus flavus*

		Water	Ethanol	Methanol	Acetone
<i>Aspergillus niger</i>	Standard antibiotic(mm)	15	15	15	15
	Control D/W	00	00	00	00
	25% (mm)	07	07	07	07
	50% (mm)	08	09	10	05
	75% (mm)	09	11	10	10
<i>Aspergillus oryzae</i>	Standard antibiotic(mm)	17	17	17	17
	Control D/W	00	00	00	00
	25% (mm)	08	07	05	06
	50% (mm)	12	10	12	08
	75% (mm)	14	12	12	12
<i>Aspergillus flavus</i>	Standard antibiotic(mm)	16	16	16	16
	Control D/W	00	00	00	00
	25% (mm)	07	13	10	08
	50% (mm)	08	13	13	09
	75% (mm)	10	16	14	10
	Standard antibiotic(mm)	14	14	14	14

Candida albicans	Control D/W	00	00	00	00
	25% (mm)	06	06	14	06
	50% (mm)	04	07	13	08
	75% (mm)	08	08	15	11
Penicillium crysogenum	Standard antibiotic(mm)	14	14	14	14
	Control D/W	00	00	00	00
	25% (mm)	06	05	08	06
	50% (mm)	08	08	10	09
	75% (mm)	09	12	12	12



fig 5 : activity against *Aspergillus oryzae*

3.7) Antimicrobial activities were also significantly inhibited in presence of A-Y, B-Y, C-Y and D-Y , viz., AY, B-Y, C-Y and D-Y, A-water, B Ethanol, C methanol & D acetone Butea monosperma AgNPs solutions (figure 6A-C and figure 6A-C)

Antimicrobial Data				
Anti-Candida activity				
	A-Y	B-Y	C-Y	D-Y

0	0.698	0.657	0.695	0.698	0.657	0.695	0.698	0.657	0.695	0.698	0.657	0.695
1.25	0.629489	0.724936	0.617458	0.553635	0.602277	0.5306	0.803338	0.749726	0.772792	0.66272	0.624762	0.540376
2.5	0.408238	0.547082	0.400168	0.300047	0.334484	0.234059	0.484978	0.535226	0.54214	0.426697	0.412055	0.340237
5	0.238873	0.319305	0.252686	0.158735	0.181607	0.126947	0.222158	0.227778	0.253286	0.236023	0.235313	0.226825
10	0.11552	0.13521	0.121918	0.121955	0.131331	0.138848	0.135873	0.140957	0.154127	0.13914	0.137694	0.124849

Anti-Proteus activity

	A-Y			B-Y			C-Y			D-Y		
0	2.548	2.534	2.177	2.548	2.534	2.177	2.548	2.534	2.177	2.548	2.534	2.177
0.62	2.877664	2.629279	2.792725	2.364163	2.669176	2.440095	2.817178	2.604826	2.830046	3.020519	3.159511	3.108032
1.25	2.160822	2.101622	1.954907	0.920183	1.002549	1.110655	2.972901	2.585521	2.967751	2.804307	2.698776	2.559782
2.5	0.697538	0.625467	0.510927	0.263829	0.280559	0.286994	2.06816	2.113204	2.090039	1.272813	1.151838	1.00641
5	0.172454	0.162158	0.163445	0.150575	0.178889	0.178889	0.236802	0.24195	0.24195	0.198193	0.193045	0.187898
10	0.136419	0.135132	0.137706	0.138993	0.137706	0.146715	0.175028	0.203341	0.200767	0.181463	0.185324	0.15701

Anti-Candida and Proteus activity

	A-Y			B-Y			C-Y			D-Y		
0	2.534	2.548	2.177	2.534	2.548	2.177	2.534	2.548	2.177	2.534	2.548	2.177
0.312	3.221147	2.741742	2.534	2.255488	2.472362	2.148193	2.266903	2.527151	2.234942	2.175587	2.257771	2.73261
0.625	2.250923	2.641295	1.94844	1.297819	1.391417	1.415387	2.126505	2.12993	2.631022	2.217821	2.126505	2.060302
1.25	1.344618	1.301243	1.103774	0.588984	0.579852	0.526205	1.397124	1.169977	1.343477	0.978215	0.955386	0.796726
2.5	0.464567	0.415485	0.386949	0.23742	0.224864	0.220298	0.644914	0.642632	0.612954	0.381242	0.382383	0.345857
5	0.198611	0.195186	0.203177	0.140397	0.138114	0.132407	0.231713	0.204318	0.227147	0.218015	0.203177	0.208884
10	0.128983	0.135832	0.13469	0.13469	0.13469	0.128983	0.162085	0.15866	0.148387	0.13469	0.148387	0.139256

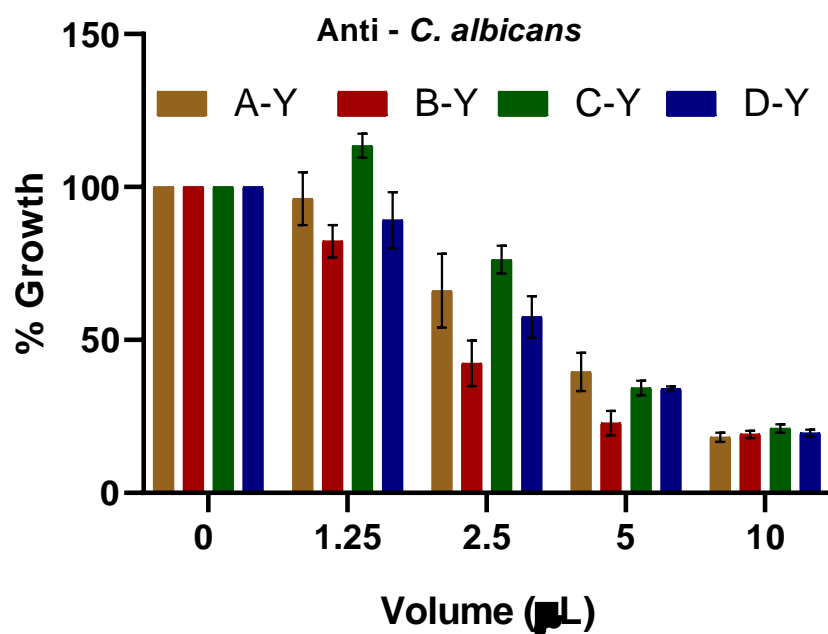


Figure 6 (A): Anti-*Candida* activity

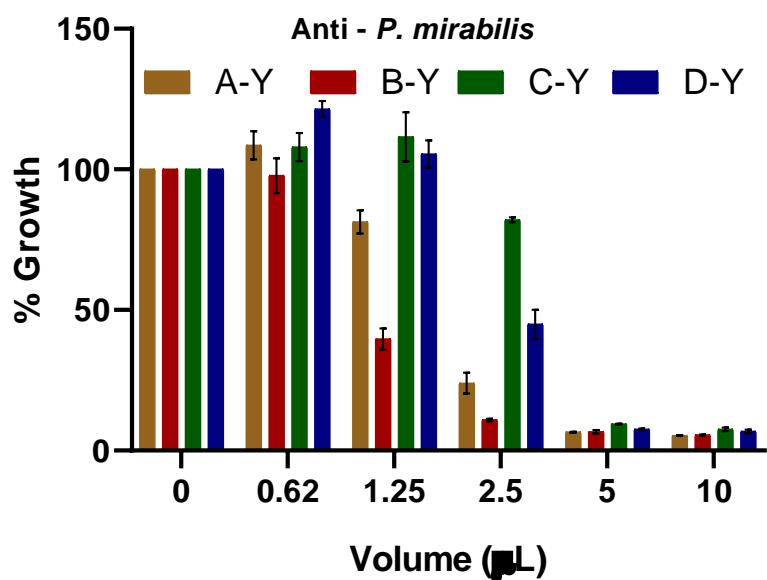


Figure 6 (B): Anti-*Protease* activity

Form the anti-microbial data, it seems that B-Y shows most potent anti-*Candida* and anti-*Protease* activity in presence of B-Y (2.5 and 1.25 μ l, respective volume).

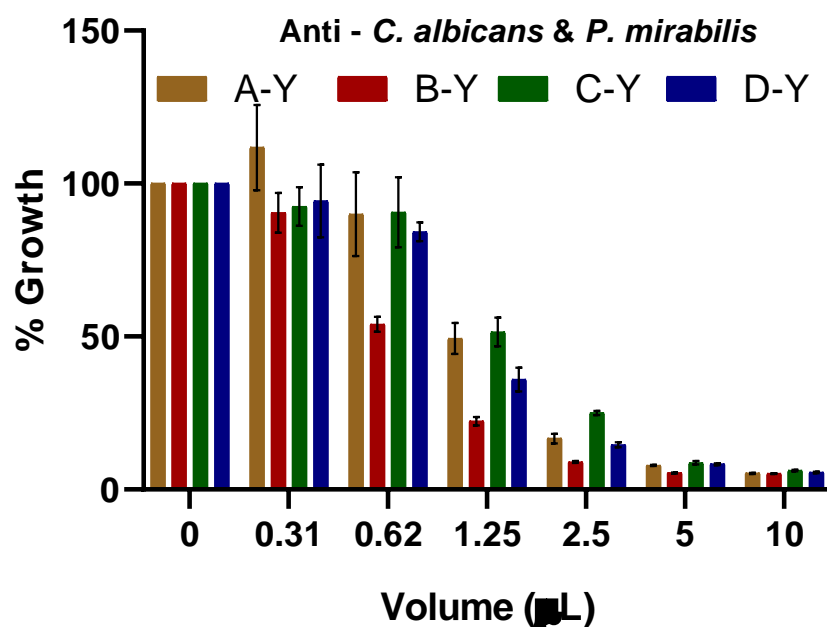


Figure 6 (C): Mixed antimicrobial activities against *Candida* and *Protease*

For mixed antimicrobial activity also, B-Y is the most antimicrobial nanoparticles inhibiting mixed growth of *Candida* and *Protease* at 1.25 μ l volume.

Other nanoparticles such as C-Y and D-Y also showed antimicrobial and antibiofilm activities but at higher volume, 5 to 10 μ l. A-water, B Ethanol, C methanol & D acetone *Butea monosperma* AgNPs solutions

Summary and Conclusion: In this research of *Butea monosperma* AgNPs solutions physical characterisation was done which identified presence of AgNPs. The spectrum has a maximum absorption peak at a wavelength which is reported to have an absorption maximum of between about 400nm to about 450nm. The presence of the maximum peak absorption peak at 400nm to about 450nm

is therefore an indication and confirmation that the AgNPs were present. FTIR spectra depicts bands at ~3200-3300 corresponding to alcoholic O-H stretching, bands at ~ 1620 corresponds to; where as small band at ~1100 is corresponds to alcoholic C-O bond, metallic silver bond is seen at ~450 cm⁻¹. Fig 2 where A-water, B Ethanol, C methanol & D acetone solvents respectively. Field Emission Scanning Electron Microscopy (Fe-SEM) & Energy Dispersive X-Ray spectroscopy (EDS) Analysis. Thin film of the as obtained sample was prepared on cleaned glass plate using drop casting technique. This film is dried under Infra-Red lamp at room temperature. As depicted in electron micrographs, sample consist of clusters of ultrafine nanoparticles of size ~40-75 nm. Fig 4 To confirm the composition of the sample, EDS analysis is done. As seen from the spectra depicted in chart 1, Sample prominently consist of Ag along with S, P, O and Si.

it was found all samples have moderate activity on above bacteria and fungus strains also have effect on mixed fungus and bacterial cultures. Form the anti-microbial data, it seems that B-Ethanol *Butea monosperma* AgNPs shows most potent anti-*Candida* and anti- *Protease* activity where as *Aspergillus Niger*, *Aspergillus Oryzae*, *Candida albicans*, *Penicillium crysogenum* and *Aspergillus flavus* are sensitive towards *Butea monosperma* AgNPs compared with standards. Antibacterial activity was evaluated by measuring the diameters of the zone of inhibitions (ZI) all the determination were performed in triplicates. *Shigella Salmonella typhi*, *Echerichia coli*, *Staphylococcus aureus*, *Pseudomonas aeruginosa*, *Acinetobacter*, *klebsiella pneumoniae*, *Bacillus*. But *klebsiella pneumoniae*, *Bacillus subtilis* were resistant to *Butea monosperma* AgNPs where as *Shigella Salmonella typhi*, *Echerichia coli*, *Staphylococcus aureus*, *Pseudomonas aeruginosa*, *Acinetobacter* were susceptible and sensitive to *Butea monosperma* AgNPs. All four solvent *Butea monosperma* AgNPs were efficient with moderate results.

References:

1. A. Y. Hwang and J. G. Gums, (2016). The emergence and evolution of antimicrobial resistance: Impact on a global scale. *Bioorganic & Medicinal Chemistry*, vol. 24, pp. 6440–6445.
2. Chi-Yu Chena, Yen-Hsu Chen, Po-LiangL,Wei-RuLinae, (2012). *Proteus mirabilis* urinary tract infection and bacteremia: Risk factors, clinical presentation, and outcomes. *Journal of Microbiology, Immunology and Infection*. Volume 45, Issue 3, Pages 228-236.
3. Kasthuri, J., Veerapandian, S., Rajendiran, N. (2009). Biological synthesis of silver and gold nanoparticles using apiin as reducing agent. *Colloids Surf. B: Biointerf.* 68, 55–60.
4. Daspute Abhijit Arun, Akash Pansande, Wagh Sopan Ganpatrao, Patil Akshay , Gangurde Anuja Suklal and Priyanka Kharpude, (2020). Effect of pomegranate (*Punica granatum* L.) peel extract on improving vase-life of cut carnation (*Dianthus caryophyllus*). *Current Horticulture* 8(2): 47–50.
5. A.R.V. Nestor, V.S. Mendieta, M.A.C. Lopez, R.M.G. Espinosa, M.A.C. Lopez and J.A.A. Alatorre Mater. (2008). Solventless synthesis and optical properties of Au and Ag nanoparticles using *Camiellia sinensis* extract. *Lett.*, 62, pp. 3103-3105
6. Tereza karla vieira lopes da costa, Mart, Carolina Medeiros de ALMEIDA, Rennaly de Freitas LIMA, Ilza maria de oliveira sousa,Elaine cristina cabral. (2018). Antifungal, antibiofilm, and antiproliferative activities of *Guapira graciliflora*. *Original Research, Microbiology Braz. oral. res.* 32.
7. D. Moonmun, R. Majumder and A. Lopamudra (2017). Quantitative Phytochemical estimation and Evaluation of antioxidant and antibacterial activity of methanol and ethanol extracts of *Heliconia rostrata*. *Indian journal of pharmaceutical sciences* 79 (1), 79-90.

8. Chitte R. R, Date P. K. and Patil A. M. (2016). Chromatographic methods for isolation and characterization of bioactive molecules from medicinal plant *Mesua ferrea* Linn. *Biochemistry and Biotechnology Research* Vol. 4(4), pp. 60-67, ISSN: 2354-2136.
9. Sindhia V. R, Bairwa R. (2010). Plant Review: *Butea monosperma*. *Int J of Pharma and Clinical Res.* 2(2): 90-94. 2
10. More B. H, Sakharwade S. N, Tembhurne S. V, Sakarkar D. M. (2012). Ethnobotany and Ethanopharmacology of *Butea Monosperma* (Lam) Kuntze- A Compressive Review. *Am J Pharm Tech Res.* 2(5): 138-159.
11. Sharma A. K, Deshwal N. (2011). An Overview: On Phytochemical and Pharmacological Studies of *Butea Monosperma*. *Int J PharmTech Res.* 3(2): 864-871.
12. Chandraker S. K. (2014). A review on endangered plant of Chhattisgarh: *Butea monosperma* (Lam.) (Parsa). *IJPRBS.* 3(3): 165-177.
13. Madhavi A. (2013). An Overview of *Butea monosperma* (Flame of Forest). *WJPPS.* 3(1): 307-319.
14. Hufford C. D., Funderburk J. M., Morgan J. M., Robertson L. W. (1975). Two antimicrobial alkaloids from heartwood of *Liriodendron tulipifera*. *I.J.pharm. Sci.*, **64**:789-792.
15. Umadevi S., Mohanta G. P., Chelladurai V., Manna P. K. and Manavalan R. (2003). Antibacterial and antifungal activity of *Andrographis echinodes*. *J. Nat. Remedies.*, **3**:185-188.
16. Khan S. and Khan G. M. (2007). *In vitro* Antifungal activity of *Rhazya stricta*, *Pak. J. Pharm. Sci.*, Vol.20(4), 274-279